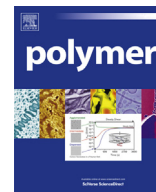




Contents lists available at ScienceDirect

Polymer

journal homepage: [www.elsevier.com/locate/polymer](http://www.elsevier.com/locate/polymer)

# Additive manufacturing with a flex activated mechanophore for nondestructive assessment of mechanochemical reactivity in complex object geometries

Bo Cao <sup>a</sup>, Nicholas Boechler <sup>b</sup>, Andrew J. Boydston <sup>a,\*</sup><sup>a</sup> Department of Chemistry, University of Washington, Seattle, WA 98195, United States<sup>b</sup> Department of Mechanical and Aerospace Engineering, University of California, San Diego, La Jolla, CA 92093, United States

## ARTICLE INFO

### Article history:

Received 27 February 2018

Received in revised form

24 April 2018

Accepted 10 May 2018

Available online xxx

### Keywords:

Additive manufacturing

Mechanochemistry

Vat photopolymerization

Lattice structures

Microstructured materials

## ABSTRACT

We used digital light processing additive manufacturing (DLP-AM) to produce mechanochemically responsive test specimens from custom photoresin formulations, wherein designer, flex activated mechanophores enable quantitative assessment of the total mechanophore activation in the specimen. The manufactured object geometries included an octet truss unit cell, a gyroid lattice, and an “8D cubic lattice”. The mechanophore activation in each test specimen was measured as a function of uniaxial compressive strain applied to the structure. Full shape recovery after compression was exhibited in all cases. These proof-of-concept results signify the potential to use flex activated mechanophore for nondestructive, quantitative volumetric assessment of mechanochemistry in test specimens with complex geometries. Additionally, the integration of DLP-AM with flex activated mechanophore build materials enabled the creation of customizable, three-dimensional mechanochemically responsive parts that exhibit small molecule release without undergoing irreversible deformation or fracture.

© 2018 Elsevier Ltd. All rights reserved.

## 1. Introduction

Mechanophores are molecular moieties that respond chemically to external mechanical stimuli [1]. In materials that contain mechanophores, macroscopic strains are translated into molecular-scale deformations at the mechanophore, which augment the potential energy surface toward specific chemical reactivity. To date, mechanophores have been demonstrated in polymers and network materials to achieve behaviors such as color change (mechanochromism) [2–4], enhanced luminescence [5], fluorescence [6], catalysis [7], self-reinforcement [8], polymer backbone structural reconfiguration [9], and small molecule release [10]. Besides molecularly designing new mechanophores that undergo force-induced bond cleavage [11], cycloreversion [12], or electrocyclic ring opening [13], efforts have been made to bridge functional mechanophores with engineering applications. For example, Zhao and coworkers fabricated electro-mechano-chemically responsive elastomeric display systems that were able to generate fluorescent patterns by coupling the mechanochemical isomerization of

spiropyran with macroscopic shape deformation caused by applied electric fields [14]. In a demonstration of autonomously self-reinforcing materials, Craig and coworkers explored polymeric materials that contained *gem*-dibromocyclopropane mechanophores, wherein spontaneous nucleophilic substitution resulted in crosslinking and strengthening of the material under otherwise destructive forces [8].

As polymer mechanochemistry continues to develop as an avenue for designing stimuli-responsive materials, one can begin to consider opportunities at the interfaces of mechanochemistry and manufacturing. One of the most rapidly developing manufacturing techniques is additive manufacturing (AM), commonly referred to as “3D printing,” which has enabled the production of complex three-dimensional (3D) structures with relative ease [15]. Recently, the fabrication of rapidly customizable mechanochromic devices was achieved through the integration of custom mechanochromic filaments with melt material extrusion AM [16,17]. These reports signified a potentially exciting opportunity to pair molecular-level strain sensitivity with custom macroscopic object geometries. As an early step toward realizing the potential of AM with mechanochemically responsive build materials, we sought a mechanophore that could quantitatively “report” activation throughout a

\* Corresponding author.

E-mail address: [ajb1515@uw.edu](mailto:ajb1515@uw.edu) (A.J. Boydston).

geometrically complex object.

In many cases, mechanophore activation is assessed through spectroscopic means, which involves either fabrication of test samples that are specific to the method of analysis, or processing of the bulk material in a way that destroys the test specimen (e.g., dissolving the material for solution-based analyses). Mechano-chromic responses can help address this challenge, but quantitative assessment is often limited to smooth, flat surfaces that are optically accessible. For instance, lattice and microstructured materials would each present formidable challenge to comprehensive assessment of mechanochromism. We hypothesized that mechanophores capable of releasing extractable, small molecules could provide a means toward quantifying mechanophore reactivity throughout the entire volume of a test specimen without requiring dissolution, digestion, or otherwise destroying the specimen. Flex activated mechanophores, such as oxanorbornadiene (OND), are potentially good candidates for such applications [18]. The OND mechanophore was previously demonstrated in bulk thermoplastics and polyurethane elastomers to release a small molecule (benzyl furfuryl ether) that could be extracted and quantified after mechanical activation (Fig. 1) [10,18]. One notable caveat is that the efficiency of extraction would be dependent upon the swelling characteristics of the bulk material and the dimensions of the test specimen. In this study, we present the first demonstration, and characterization, of 3D structures with complex object geometries fabricated via AM, which incorporate a flex activated mechanophore that enables the quantitative assessment of mechanophore activation within mechanically reversible regimes.

## 2. Results and discussion

We first selected an appropriate AM method based on the intended target geometries of our test specimens (e.g. lattice materials) and the inherent reactivity of the OND mechanophore. The desire to have overhangs and void spaces within lattice designs prompted the use of vat photopolymerization [19]. Moreover, the general thermal instability of OND substrates was likely to preclude melt material extrusion. As a subset of vat photopolymerization, we applied digital light processing additive manufacturing (DLP-AM) in our studies to enable efficient printing with visible light [20], therefore also avoiding photochemical degradation of the OND that

occurs upon exposure to UV light [21]. Previous success with customizable photoresins for DLP-AM, including the production of elastomeric and graded materials, encouraged the possibility of incorporating an appropriately functionalized OND mechanophore [22,23]. The stability of the OND moiety within the DLP-AM process was examined by irradiating an OND-diol in deuterated chloroform ( $\text{CDCl}_3$ ) solution with white light from the projector used during the AM process. After 2 h of exposure to the projector light, the NMR spectrum (Figure S1) showed no changes in comparison with the pristine OND-diol. This result suggested that the AM conditions would not cause photochemical degradation of the OND moiety.

To incorporate oxanorbornadiene chemically into crosslinked polymer networks during the DLP-AM process, we prepared an oxanorbornadiene-dimethacrylate (OND-DMA) as previously described [10]. This structure enables crosslinking during photocuring with the mechanophore positioned within the bridging network segment, such that the mechanical strain can be transduced into chemical potential. The complete photoresin was comprised of 98.52 wt % of 2-hydroxyethyl acrylate (HEA), 0.49 wt % of Irgacure 819 as photoinitiator, and 0.99 wt % of OND-DMA. Additionally, 0.01 wt % of Nile Red was added to the resin as a light absorber to decrease the outgrowth during AM. The DLP-AM setup is diagrammed in Figure S2 and the schematic of the layer-by-layer printing process is shown in Figure S3, illustrating the direct formation of the mechanophore-containing polymer networks from liquid resins.

To investigate the printability of the resin and characterize the mechanical properties of the printed material, dogbone tensile test specimens (dimensions: 63.5 mm  $\times$  9.53 mm  $\times$  3.20 mm) were printed and evaluated via uniaxial tension tests. We first investigated the effects of layer cure time on the printed material's mechanical properties by the measuring the load as a function of monotonically increasing strain until the point of specimen fracture. As presented in Fig. 2a, the stress-strain curves of test specimens printed with layer cure times ranging from 5 s to 11 s showed similar mechanical behavior. The tests specimens also demonstrated a significant elongation at break, with strains ranging from 156% to 188% (Fig. 2b, elongation measured by tracking two marks made within the specimen's gauge region using a video extensometer). The gel fraction of a representative disc-shaped sample was determined by performing Soxhlet extraction (detailed

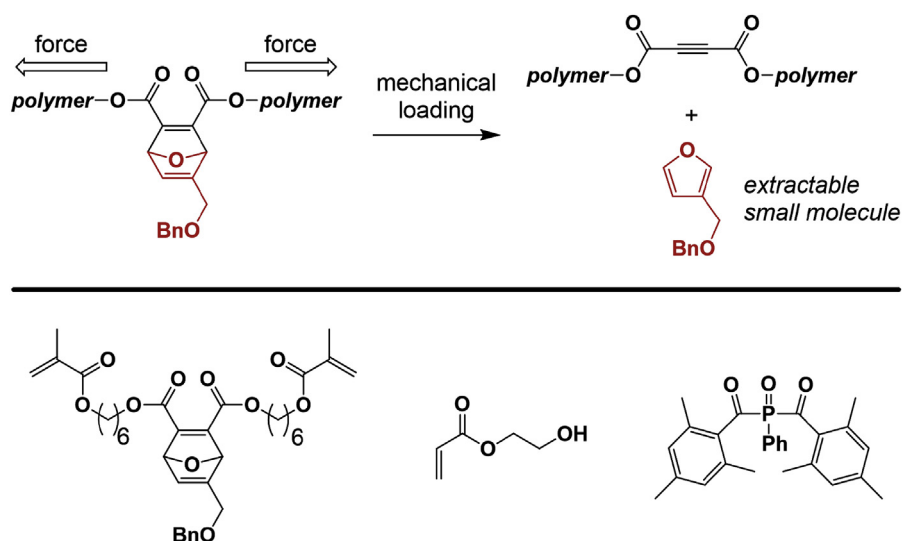
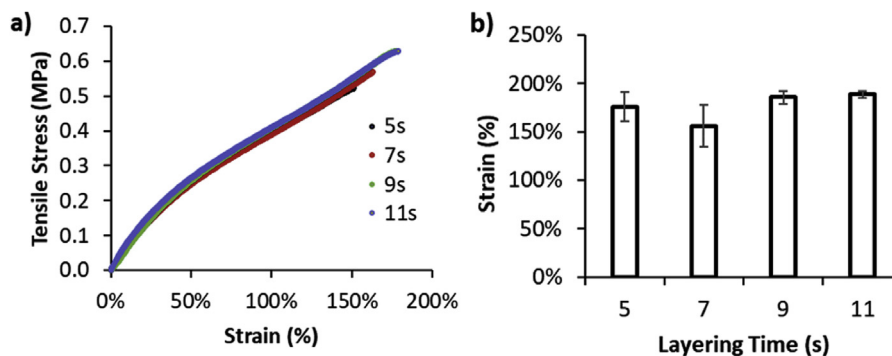


Fig. 1. (top) Generalized depiction of mechanochemical flex activation of an oxanorbornadiene under mechanical load. (bottom) Chemical structures of components of the photoresin formulation used in this study; left-to-right: OND mechanophore, 2-hydroxyethyl acrylate (HEA), Irgacure 819.



**Fig. 2.** a) Representative tensile test results for printed specimens (ASTM D638 Type V, strain rate = 20 mm/min, gauge length = 9.53 mm) at different layer cure times (5s, 7s, 9s, and 11s), b) Strain at break for printed specimens at different layer cure times. Error bars represents standard deviation over three samples.

procedures included in the Supporting Information) and found to be 97.7%, suggesting high efficiency of crosslinking during the printing process. These results are consistent with our previous investigations of HEA-based photoresins for DLP-AM [22].

The persistence of the mechanochemical reactivity after additive manufacturing was investigated by printing thin slabs (dimensions: 29.32 mm × 29.32 mm × 1.00 mm) using the prepared resins. The slabs were cut into small pieces, placed into a die set, and then compressed uniaxially using an Instron 5585H Universal Testing System. Bulk compression at sustained pressures, as indicated in Fig. 3, was held for 1 min. The samples were then soaked in hexane for 24 h to extract the released benzyl furfuryl ether. During extraction, the samples were found to swell and remain intact. The extract was then analyzed by gas chromatography mass spectrometry (GC-MS) using an internal standard. The percent activation of the flex-activated mechanophore was calculated based on the amount of released small molecules versus the initial feed ratio of the OND-DMA in the resin [18]. As can be seen in Fig. 3, the 3D printed slabs showed a low amount of background activation (ca. 0.52%) without compression. A monotonic increase in the activation, up to ca. 2.47%, was observed with applied pressure of up to 125 MPa. The observed mechanochemical profile of these materials are similar to those previously reported, and consistent with mechanical impetus as the driving force for the reaction [10,18]. Moreover, the OND mechanophore does not give false positive results during the applied GC-MS protocol, consistent with our previous studies of this system [10,18].

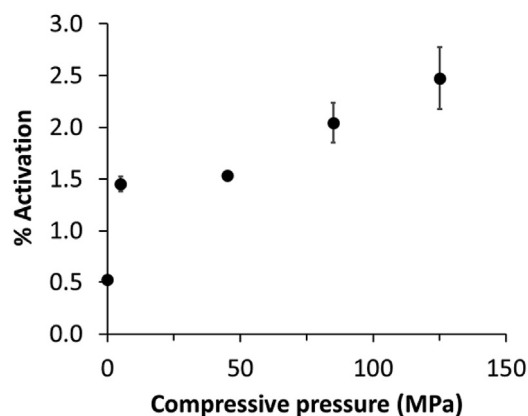


**Fig. 3.** Plot of % mechanophore activation in a printed specimen (cut, printed slabs) versus applied pressure, as judged by GC-MS analysis of extract solutions after compression. Error bars represent the standard deviation over three samples.

Having successfully confirmed the mechanochemical reactivity of the mechanoresponsive materials after DLP-AM, we targeted more complex object geometries for the test specimens. Specifically, we investigated an octet truss unit cell (exterior dimensions: 14.66 mm × 14.66 mm × 14.66 mm) [24,25], an “8D cubic lattice” (exterior dimensions: 17.74 mm × 17.74 mm × 18.75 mm) [26], and a gyroid lattice (exterior dimensions: 14.91 mm × 14.91 mm × 12.34 mm) architecture [27]; representative printed specimens are depicted in Fig. 4. The printed samples were uniaxially compressed in the Instron load frame to 20%, 40%, 60%, and 80% global strain (compression details and images are shown in the Supporting Information), where the definition of “global strain” is the compression of the entire structure divided by the original height. The octet truss unit cell and 8D cubic lattice specimens each displayed visible buckling during the course of compression, which was also expected for the gyroid lattice specimens though it was not easy. Each of the samples fully recovered to their original shape without visibly observable fracture or failure of any structural components.

As in the case of the cut, printed slabs, without compression, each specimen type displayed relatively low mechanophore activation. While the activation of the cut slabs might be attributed to the deformation induced by cutting the slabs, this effect would not be present in the specimens shown in Fig. 4, and as such, we suggest this baseline activation may be ascribed to thermal activation during printing or solvent-induced swelling during the extraction protocol. Upon uniaxial compression, the mechanophore-containing objects revealed increasing levels of mechanophore activation with increasing applied global strain (Fig. 4). Specifically, mechanophore activation in the octet truss unit cells increased from 0.32% to 0.99% when the global strain was increased from 0 to 80%. The 8D cubic lattice and gyroid lattice samples each displayed slightly greater maximum activation (1.57% and 1.68%, respectively) in comparison with the octet truss unit cell. Notably, the octet truss unit cell and gyroid lattice displayed similar activation-strain profiles, with steep increases near 60%–80% strain. These observations are consistent with the applied force profiles measured for each object geometry (Figures S5 and S7), which exhibit a stiffening within this strain region that would be consistent with densification of, and the onset of self-contact within, the lattice (Figure S8). However, it is thus far unclear within the context of this explanation as to why the 8D cubic lattice does not exhibit a similar increase in mechanophore activation slope, particularly given the similar applied force profiles (Figure S6). These results highlight the sensitivity of the mechanophores to behave as local, molecular-level strain probes that respond to different local strains generated as a result of the object's unique geometry and mechanical behavior.

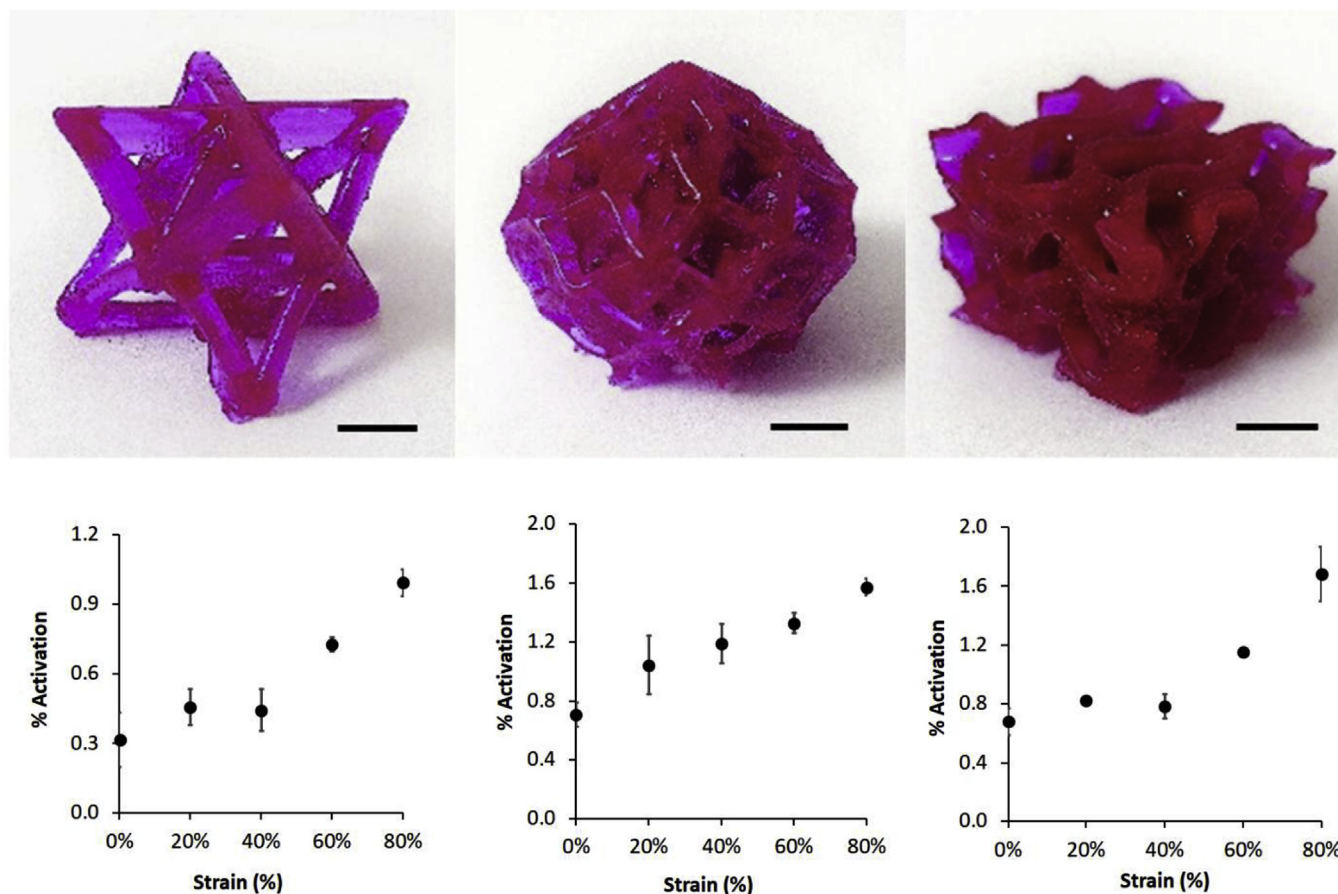


Fig. 4. Top, left-to-right: As printed octet truss unit cell, 8D cubic lattice, and gyroid lattice. Bottom, left-to-right: plot of % activation of mechanophore after compression of octet truss unit cell specimens, 8D cubic lattice specimens, and gyroid lattice specimens. Error bars represent standard deviation over three samples. Scale bars = 5 mm.

### 3. Conclusions

In summary, we have confirmed the compatibility of a flex activated OND mechanophore with DLP-AM techniques. To our knowledge, this is the first demonstration of AM with a flex activated mechanophore. The OND mechanophore was incorporated into an elastomer photocurable resin that resulted in good printing characteristics for a series of microstructured test specimens. This enabled investigation of the force-induced small molecule release characteristics of the printed material by bulk compression studies. Moreover, the differing extents of mechanophore activation observed for several complex geometries created by DLP-AM open a new avenue for using this mechanophore to explore the strain distribution in sophisticated 3D architectures and the tailoring of mechanochemical activation via designed object geometry.

### Acknowledgements

We gratefully acknowledge financial support from the Army Research Office (Grant No. W911NF-15-1-0139 and W911NF-17-1-0595). We thank Professors Duane Storti (University of Washington), Mark Ganter (University of Washington), Alshakim Nelson (University of Washington), and Stephen Craig (Duke University) for helpful discussions.

### Appendix A. Supplementary data

Supplementary data related to this article can be found at

<https://doi.org/10.1016/j.polymer.2018.05.031>.

### References

- [1] J. Li, C. Nagamani, J.S. Moore, Polymer mechanochemistry: from destructive to productive, *Acc. Chem. Res.* 48 (2015) 2181–2190, <https://doi.org/10.1021/acs.accounts.5b00184>.
- [2] D.A. Davis, A. Hamilton, J. Yang, L.D. Cremar, D. Van Gough, S.L. Potisek, M.T. Ong, P.V. Braun, T.J. Martinez, S.R. White, J.S. Moore, N.R. Sottos, Force-induced activation of covalent bonds in mechanoresponsive polymeric materials, *Nature* 459 (2009) 68–72, <https://doi.org/10.1038/nature07970>.
- [3] M.J. Robb, T.A. Kim, A.J. Halmes, S.R. White, N.R. Sottos, J.S. Moore, Regioisomer-specific mechanochromism of naphthopyran in polymeric materials, *J. Am. Chem. Soc.* 138 (2016) 12328–12331, <https://doi.org/10.1021/jacs.6b07610>.
- [4] K. Imato, A. Irie, T. Kosuge, T. Ohishi, M. Nishihara, A. Takahara, H. Otsuka, Mechanophores with a reversible radical system and freezing-induced mechanochemistry in polymer solutions and gels, *Angew. Chemie Int. Ed* 54 (2015) 6168–6172, <https://doi.org/10.1002/anie.201412413>.
- [5] Y. Chen, A.J.H. Spiering, S. Karthikeyan, G.W.M. Peters, E.W. Meijer, R.P. Sijbesma, Mechanically induced chemiluminescence from polymers incorporating a 1,2-dioxetane unit in the main chain, *Nat. Chem.* 4 (2012) 559–562, <https://doi.org/10.1038/nchem.1358>.
- [6] G.R. Gossweiler, G.B. Hewage, G. Soriano, Q. Wang, G.W. Welshofer, X. Zhao, S.L. Craig, Mechanochemical activation of covalent bonds in polymers with full and repeatable macroscopic shape recovery, *ACS Macro Lett.* 3 (2014) 216–219, <https://doi.org/10.1021/mz500031q>.
- [7] A. Piermattei, S. Karthikeyan, R.P. Sijbesma, Activating catalysts with mechanical force, *Nat. Chem.* 1 (2009) 133–137, <https://doi.org/10.1038/nchem.167>.
- [8] A.L.B. Ramirez, Z.S. Kean, J.A. Orlicki, M. Champhekar, S.M. Elsagr, W.E. Krause, S.L. Craig, Mechanochemical strengthening of a synthetic polymer in response to typically destructive shear forces, *Nat. Chem.* 5 (2013) 757–761, <https://doi.org/10.1038/nchem.1720>.
- [9] Z. Chen, J.A.M. Mercer, X. Zhu, J.A.H. Romaniuk, R. Pfattner, L. Cegelski, T.J. Martinez, N.Z. Burns, Y. Xia, Mechanochemical unzipping of insulating

- poly(adderene) to semiconducting polyacetylene, *Science* 357 (2017) 475–479, <https://doi.org/10.1126/science.aan2797>.
- [10] M.B. Larsen, A.J. Boydston, “Flex-activated” mechanophores: using polymer mechanochemistry to direct bond bending activation, *J. Am. Chem. Soc.* 135 (2013) 8189–8192, <https://doi.org/10.1021/ja403757p>.
- [11] I. Park, S.S. Sheiko, A. Nese, K. Matyjaszewski, Molecular tensile testing machines: breaking a specific covalent bond by adsorption-induced tension in brushlike macromolecules, *Macromolecules* 42 (2009) 1805–1807, <https://doi.org/10.1021/ma8026996>.
- [12] H.M. Klukovich, Z.S. Kean, S.T. Iacono, S.L. Craig, Mechanically induced scission and subsequent thermal remending of perfluorocyclobutane polymers, *J. Am. Chem. Soc.* 133 (2011) 17882–17888, <https://doi.org/10.1021/ja2074517>.
- [13] C.K. Lee, D.A. Davis, S.R. White, J.S. Moore, N.R. Sottos, P.V. Braun, Force-induced redistribution of a chemical equilibrium, *J. Am. Chem. Soc.* 132 (2010) 16107–16111, <https://doi.org/10.1021/ja106332g>.
- [14] Q. Wang, G.R. Gossweiler, S.L. Craig, X. Zhao, Cephalopod-inspired design of electro-mechano-chemically responsive elastomers for on-demand fluorescent patterning, *Nat. Commun.* 5 (2014) 4899, <https://doi.org/10.1038/ncomms5899>.
- [15] M. Hofmann, 3D printing gets a boost and opportunities with polymer materials, *ACS Macro Lett.* 3 (2014) 382–386, <https://doi.org/10.1021/mz4006556>.
- [16] G.I. Peterson, M.B. Larsen, M.A. Ganter, D.W. Storti, A.J. Boydston, 3D-Printed mechanochromic materials, *ACS Appl. Mater. Interfaces* 7 (2015) 577–583, <https://doi.org/10.1021/am506745m>.
- [17] G.I. Peterson, M. Yurtoglu, M.B. Larsen, S.L. Craig, M.A. Ganter, D.W. Storti, A.J. Boydston, Additive manufacturing of mechanochromic polycaprolactone on entry-level systems, *Rapid Prototyp. J.* 21 (2015) 520–527, <https://doi.org/10.1108/RPJ-09-2014-0115>.
- [18] M.B. Larsen, A.J. Boydston, Successive mechanochemical activation and small molecule release in an elastomeric material, *J. Am. Chem. Soc.* 136 (2014) 1276–1279, <https://doi.org/10.1021/ja411891x>.
- [19] J.-Y. Lee, J. An, C.K. Chua, Fundamentals and applications of 3D printing for novel materials, *Appl. Mater. Today* 7 (2017) 120–133, <https://doi.org/10.1016/j.apmt.2017.02.004>.
- [20] J. Wallace, M.O. Wang, P. Thompson, M. Busso, V. Belle, N. Mammoser, K. Kim, J.P. Fisher, A. Siblani, Y. Xu, J.F. Welter, D.P. Lennon, J. Sun, A.I. Caplan, D. Dean, Validating continuous digital light processing (cDLP) additive manufacturing accuracy and tissue engineering utility of a dye-initiator package, *Biofabrication* 6 (2014) 15003, <https://doi.org/10.1088/1758-5082/6/1/015003>.
- [21] M. Bohle, R.M. Borzilleri, D. Döpp, H. Döpp, R.J. Herr, *Science of Synthesis: Houben-weyl Methods of Molecular Transformations*, vol. 17, Georg Thieme Verlag, 2014, p. 632.
- [22] C.J. Thrasher, J.J. Schwartz, A.J. Boydston, Modular elastomer photoresins for digital light processing additive manufacturing, *ACS Appl. Mater. Interfaces* (2017) 39708–39716, <https://doi.org/10.1021/acsami.7b13909>.
- [23] G.I. Peterson, J.J. Schwartz, D. Zhang, B.M. Weiss, M.A. Ganter, D.W. Storti, A.J. Boydston, Production of materials with spatially-controlled cross-link density via vat photopolymerization, *ACS Appl. Mater. Interfaces* 8 (2016) 29037–29043, <https://doi.org/10.1021/acsami.6b09768>.
- [24] R.B. Fuller, R.B., Synergetic Building Construction, U.S. Patent Serial No. 2, 986, 241 (1961).
- [25] V.S. Deshpande, N.A. Fleck, M.F. Ashby, Effective properties of the octet-truss lattice material, *J. Mech. Phys. Solids* 49 (2001) 1747–1769.
- [26] chriskpalmer, 8D cubic lattice (3D shadow), Sept. 8, [www.thingiverse.com/thing:30001](http://www.thingiverse.com/thing:30001), 2012.
- [27] A.H. Schoen, Infinite periodic minimal surfaces without self-intersections, *NASA Tech. Note* (1970) 1–98. TN D-5541.